Theoretical and experimental study of organic fouling of loose nanofiltration membrane

Wenyuan Ye[a], Nicole J. Bernstein[b], Jiuyang Lin[c,d]*, Jeroen Jordens[d], Shuaifei Zhao[e], Chuyang Y. Tang[f], Bart Van der Bruggen[d]

* Corresponding author: linjiuyang@126.com (J. Lin).

[a] *Fujian Provincial Key Laboratory of Soil Environmental Health and Regulation, College of Resources and Environment, Fujian Agriculture and Forestry University, Fuzhou 350002, China*

[b] *Department of Chemical Engineering, Pennsylvania State University, University Park, PA 16802, USA*

[c] *School of Environment and Resources, Qi Shan Campus, Fuzhou University, No. 2 Xueyuan Road, University Town, 350116 Fuzhou, Fujian, China*

[d] *Department of Chemical Engineering, Process Engineering for Sustainable Systems (ProcESS), KU Leuven, Celestijnenlaan 200F, B-3001 Leuven, Belgium*

[e] *Department of Environmental Sciences, Faculty of Science and Engineering, Macquarie University, Sydney, NSW 2109, Australia*

[f] *Department of Civil Engineering, The University of Hong Kong, Pokfulam HW619B, Hong Kong*

Abstract: Loose nanofiltration (NF) membranes are an attractive avenue in effective separation of organic matters and salts for resource recovery from highly-loaded wastewater. However, membrane fouling remains an unclear and complex factor in practical applications. In this work, the flux of a loose NF membrane fouled by humic acid at various solution compositions was systematically investigated. The strong hydrophilicity of the loose NF membrane allows for slight deposition of humic acid on the membrane surface, yielding an outstanding antifouling performance. However, a moderate flux decline was observed at low pH and high ionic strength, due to reduction in charge density of membrane surface for formation of a porous foulant layer. At higher ionic strength, cake-enhanced concentration polarization was the fouling mechanism that dominates the membrane flux. The presence of calcium ions induced bridging between humic acid molecules to generate a compact foulant layer, tremendously deteriorating the membrane flux. Based on COMSOL simulation for the membrane module, the hydrodynamics near the membrane surface had a more significant effect on membrane fouling than the solution chemistry, which is consistent with scanning electronic microscopy observation. This indicates benign hydrodynamic condition can be an effective strategy to fouling control for loose NF membranes.

Keywords: Loose NF membrane; Humic acid; Organic fouling; Hydrodynamics; COMSOL simulation

1. Introduction

Water scarcity and contamination severely hamper the sustainable development of the modern global society, and are the critical challenges of the 21st century [1,2]. A sustainable access to clean water is a strategic solution to these challenges. Nanofiltration (NF) emerges as an advanced separation technology for the removal of organic micro-pollutants (i.e., pharmaceuticals, endocrine disrupting compounds, and pesticides) from groundwater, surface water and seawater, based on the synergistic effect of size exclusion and electrostatic repulsion [3-6]. In particular, loose NF membranes retaining compounds in the range of 500~1000 Da are of interest as a state-of-the-art technology, which allows for sufficient fractionation of organics/salt mixtures with an acceptably high permeation flux, due to the loose surface structure, which facilitates the salt transmission and reduces concentration polarization effect [7-13].

Loose NF membranes show a vast potential for wastewater treatment, i.e., dye or antibiotics removal, in view of resource extraction and water reclamation [14-18]. For instance, Da et al. developed an yttria-stabilized-zirconia loose NF membrane through the sol-gel process, presenting 99% dye retention and ~98% NaCl removal [15]. The sulfonated thin-film composite nanofiltration membrane through interfacial polymerization of 2,2′-benzidinedisulfonic acid and trimesoyl chloride displayed over 99% rejection for Congo red, but extremely low retention (<1.8%) for NaCl, which tremendously outperforms commercial NF 270 membrane for dye desalination [19]. The novel loose NF membrane designed by bio-inspired co-deposition of polydopamine and copper nanoparticles yielded an extremely high rejection for dye molecules and fast transport of NaCl, with strong antimicrobial property [10]. Furthermore, Cheng et al. developed a loose NF membrane through bio-inspired coating of gallic acid and branched

polyethyleneimine, yielding a 96.7% rejection to Azithromycin [17]. Unfortunately, fouling caused by organic matters is a ubiquitous problem across all applications of NF technology, which substantially deteriorates the membrane flux and permeate quality.

In the past decades, comprehensive investigations on organic fouling of commercially available (tight) NF membranes, i.e., NF 90 from Dow-Filmtec (MWCO of 200 Da), NE 70 from Saehan (MWCO of ~350 Da), and NP030 from Microdyn-Nadir (MWCO of 400 Da), that retain compounds in the range of 100~500 Da were conducted, revealing the critical fouling-related factors, i.e., solution chemistry, hydrodynamic conditions, and membrane properties [20-28]. However, the fouling behavior of loose NF membranes is not well documented, failing to serve as guideline for their industrial application. Therefore, a systematical investigation for understanding organic fouling of loose NF membranes is of great significance in broadening their applications in drinking water production, brackish water and seawater desalination, and wastewater treatment.

This study aims to understand the effects of the solution chemistry and hydraulic conditions on organic fouling and solute rejection of a loose NF membrane (i.e., Sepro NF 6 with MWCO of 862 Da, Ultura). Specifically, the dependence of flux behavior and solute rejection on humic acid concentration, pH, ionic strength, calcium concentration and magnesium concentration was investigated. Furthermore, the interactions between the membrane surface, organic foulants and inorganic solutes at different hydraulic conditions were validated by COMSOL simulation and scanning electronic microscopy (SEM) observation.

2. Experimental

2.1 Materials

The model foulants including humic acid, sodium alginate and bovine serum albumin (BSA) were obtained in powder form from Sigma Aldrich (Belgium). Specifically, 2 $g \cdot L^{-1}$ humic acid, sodium alginate and BSA solutions were prepared as storage solution. The pH and ionic compositions of the feed solution were adjusted by the addition of hydrochloric acid, sodium hydroxide, sodium chloride (NaCl) or calcium chloride ($CaCl_2$). MilliQ water (electrical resistance of 18.2 MΩ·cm, Millipore, USA) was used throughout the experiments. Working solutions were freshly prepared prior to each fouling experiment. Unless otherwise specified, all the reagents were used as received.

A loose thin film composite NF membrane (Sepro NF 6, Ultura, USA) with poly-piperazineamide chemistry and high hydrophilicity was investigated in the current study. Its properties are summarized in Table 1.

Table 1 Properties of the selected loose NF membrane in this study [29]

Membrane	PWP ($L \cdot m^{-2} \cdot h^{-1} \cdot bar^{-1}$)[a]	MWCO (Da)	NaCl rejection (%)[b]	Isoelectric point	Water contact angel (°)	R_{rms} (nm)[c]
Sepro NF 6	16.6 ± 0.7	862	5.33	5.1	14.3±0.9	6.31

[a] PWP denotes pure water permeability;

[b] Rejection of 10 $g \cdot L^{-1}$ NaCl solution at 6 bar and 25°C;

[c] R_{rms} denotes root mean square roughness.

2.2 Membrane performance tests

Fouling performance of the loose NF membrane was evaluated with a lab-scale cross-flow permeation cell (Fig. 1). Briefly, before the experiment, flat sheet membrane coupons (7.0 cm × 7.0 cm) were soaked in MilliQ water for 24 h, and then loaded in the membrane module for pre-compaction by filtering MilliQ water at 8 bar to obtain a steady-state flux.

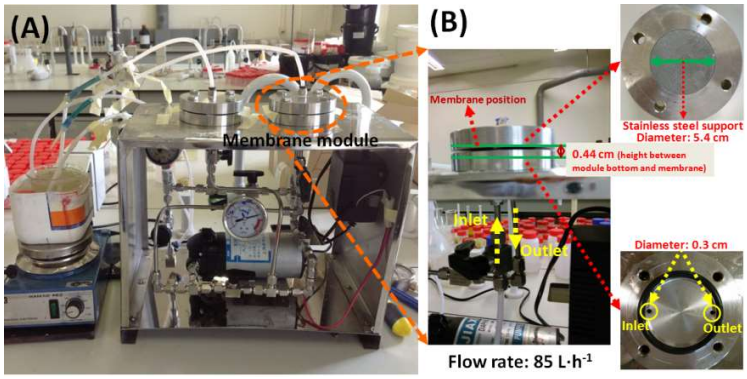

Fig. 1 Digital photo of NF membrane setup (A) and dimension of the membrane module (B)

Afterwards, the foulants with different concentrations (e.g., humic acid solution of 20, 50, and 100 ppm; sodium alginate solution of 20, 50, 100, and 200 ppm; BSA solution of 50, 200, 500, and 1000 ppm) were introduced in the feed solution and then the filtration performance of the NF membrane was performed in recirculation mode at 6 bar and 25±1 °C. The cross flow rate of the NF setup was set to 85 $L \cdot h^{-1}$. Furthermore, the effect of pH, ionic strength, and divalent Ca^{2+} ions on the fouling behavior of the loose NF membrane caused by humic acids was systematically investigated at the same operating conditions. In order to test the flux and solute rejection, samples of the feed solution and permeate were taken in fixed time intervals.

2.3 Flux and solute rejection

The permeation flux (J) was determined from the time interval to collect a fixed volume of water at 6 bar using the following equation:

$$J = \frac{V}{A \cdot t} \tag{1}$$

where V is the water volume collected during the time interval t and A denotes the effective membrane area for water permeation.

Generally, NF membranes are subject to fouling and concentration polarization. In order to investigate the fouling mechanism of the loose NF membrane, the theoretical flux was calculated

at the assumption that no interaction between inorganic salt and organic foulants occurs. Taking these phenomena into consideration, the theoretical permeation flux (J_w) can be expressed by a resistance-in-series model, given in Eq. 2 [8]:

$$J_W = \frac{\Delta P - \Delta\pi}{\mu\left(R_m + R_f + R_{cp}\right)} \tag{2}$$

where ΔP represents the transmembrane pressure, $\Delta\pi$ denotes the osmotic pressure difference between the bulk and permeate solution, μ represents the viscosity of the feed solution, R_m is the intrinsic membrane resistance, R_f denotes the hydraulic resistance caused by fouling, such as cake layer formation and pore blocking, and R_{cp} is the resistance induced by concentration polarization of inorganic salts.

For a multi-component solution, the osmotic pressure difference ($\Delta\pi$) is calculated by superimposing the contribution from each individual component, expressed as [30]:

$$\Delta\pi = \sum_{i=1}^{i=n} \Delta\pi_i = \Delta\pi_1 + \Delta\pi_2 + \Delta\pi_3 + \cdots + \Delta\pi_n \tag{3}$$

For the dilute solution, the osmotic pressure can be determined by the Van't Hoff equation:

$$\pi_i = C_i R_g T \tag{4}$$

where C_i is the molarity of solute, R_g is the universal gas constant, and T is the thermodynamic (absolute) temperature.

Furthermore, the observed rejection coefficient (R) of different solutes can be calculated as

$$R(\%) = \frac{C_f - C_p}{C_f} \times 100 \tag{5}$$

where C_f and C_p are the solute concentration in the feed and permeate, respectively.

In Eq. 2, the value of R_m for Sepro NF 6 membrane was calculated from the flux of pure water; the value of R_f was determined from individual filtration using humic acid solution without salt addition, and the value of R_{cp} was fixed by independent filtration of NaCl solutions.

2.4 Membrane characterization

The surface morphology of the tested loose NF membrane after the fouling was visualized by SEM measurement with a Philips Scanning Electron Microscope XL30 FEG (the Netherlands). The samples were dried prior to analysis in a vacuum chamber, and then sputter-coated with gold nanoparticles. The SEM images were taken at 5000x magnification in high vacuum condition.

2.5 Analytical methods

The concentration of humic acid was determined by a Shimadzu UV-1601 double beam spectrophotometer (Japan) at the wavelength of 254 nm through Lambert-Beer's Law. The concentration of Na^{+}, Mg^{2+}, and Ca^{2+} ions in the feed and permeate was determined by ICP-MS (Thermo Electron Corporation X series). Gallium (69Ga) and Indium (115In) were applied as internal standards to minimize the matrix interference and instrumental drift. The zeta potential of humic acid solutions was measured by Nanobrook Omni analyser (Nanobrook Omni, Brookhaven, US). Each sample was measured by three times, and average values are reported.

3. COMSOL Simulation

Generally, membrane fouling remains an inevitable challenge associated with membrane processes in large industrial modules as well as in small bench-scale cells [31]. Specifically, the flow behavior in the membrane system is substantially related to the filtration performance of nanofiltration membranes [32-34]. Therefore, the implementation of computational fluid dynamics (CFD) is an asset to understand the flow behavior in the membrane module or on the membrane surface.

In this work, the crossflow filtration cell for NF in CFD simulation is a circular cell, constructed of stainless steel with a chamber thickness of 0.44 mm and a diameter of 5.4 cm (Fig. 1B). The feed chamber has a feed inlet and a retentate outlet with a 3 mm diameter. In this case, the feed in the membrane module remains isothermal (25±1 °C). The effect of components (humic acid and

salt) present in the feed solution on the viscosity or density of the liquid is negligible, due to the low contents. Therefore, the flow profile in the membrane module can be described by the Navier-Stokes equation [31,34,35]:

$$\rho\left(\frac{\partial \bar{u}}{\partial t}+\bar{u}\nabla\bar{u}\right)=-\nabla p+\mu\nabla^2\bar{u} \tag{6}$$

where $\bar{u}$ is the flow velocity, p is the pressure, μ denotes the dynamic viscosity, and ρ presents the density of the feed solution. The density and dynamic viscosity for water were obtained from the material database provided by COMSOL Multiphysics 5.1 software package. In this simulation, the Laminar Flow module was used to simulate the flow velocities and profile in 3D. The applied 3D grid consists of a physics controlled mesh of free tetrahedral elements with a maximum element size of 1.04 mm. A convergence criteria of 10^{-3} was used. The no-slip ($\bar{u}$=0) boundary condition is set at all walls except for the inlet and outlet. At the inlet of the membrane module, the flow velocity is set to be equal to the average laminar flow velocity $\bar{u}$=-$\bar{n}U_0$, where $\bar{n}$ is the boundary normal pointing out of the domain and U_0 presents the normal inlet velocity. At the outlet of the membrane module, the Dirichlet condition p=0 is assumed and backflow is suppressed. Fig. 2 shows the velocity profile in the membrane module at different inlet flow rates (i.e., 55, 70 and 85 L·h^{-1}).

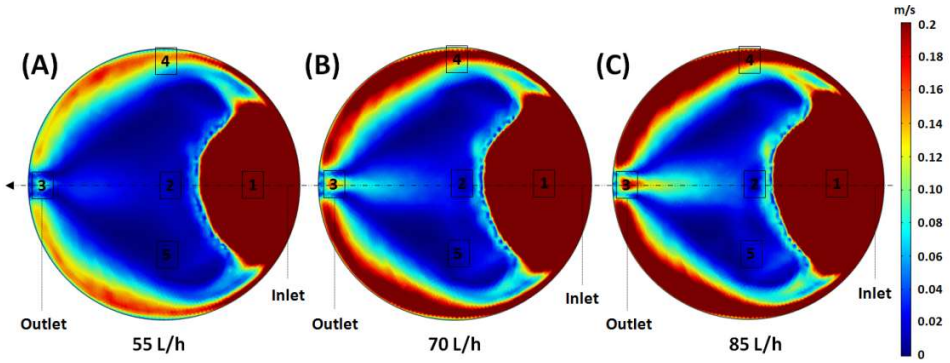

Fig. 2 Velocity profiles in the membrane module at different inlet flow rates. (A): 55 L·h^{-1}; (B): 70 L·h^{-1}; (C): 85 L·h^{-1}.

As indicated in Fig. 2, the velocity in the membrane module shows a significant improvement with increasing inlet flow rates. Noticeably, the observed “lung” shape presents the low velocity zone, which potentially suffers from the propensity of membrane fouling. At the other locations, especially the inlet and outlet (Zones 1 and 3), better hydrodynamic conditions can be achieved. To minimize membrane fouling, a high flow rate (i.e., 85 $L \cdot h^{-1}$) was adopted for the experiments in this case, as described in Section 2.2.

4. Results and discussion

4.1 Effect of foulant concentration

The filtration of a humic acid solution with different concentrations using Sepro NF 6 in is shown in Fig. 3.

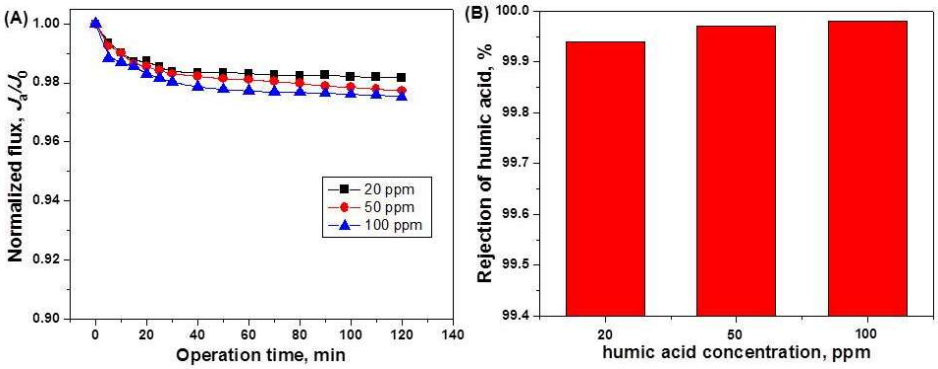

Fig. 3 Flux (A) and solute rejection (B) of Sepro NF 6 with different humic acid concentrations

As indicated in Fig. 3, humic acid has no significant effect on the flux of a loose NF membrane. Although frequent collisions of humic acid molecules onto the membrane surface occur with increasing humic acid concentrations [21], a slight flux decline for Sepro NF 6 was observed without sacrificing the humic acid rejection (>99.9%). This is mainly due to the strong hydrophilicity of the membrane surface, which minimizes the deposition of humic acids, yielding a normalized flux of 97.3% over the entire duration of the operation. On the other hand, with the

absence of other ionic species (e.g., Na^{+}, Mg^{2+} and Ca^{2+}), the weak foulant-foulant interaction induces the formation of a loose cake layer of humic acids on the membrane surface (Fig. 4), alleviating membrane fouling.

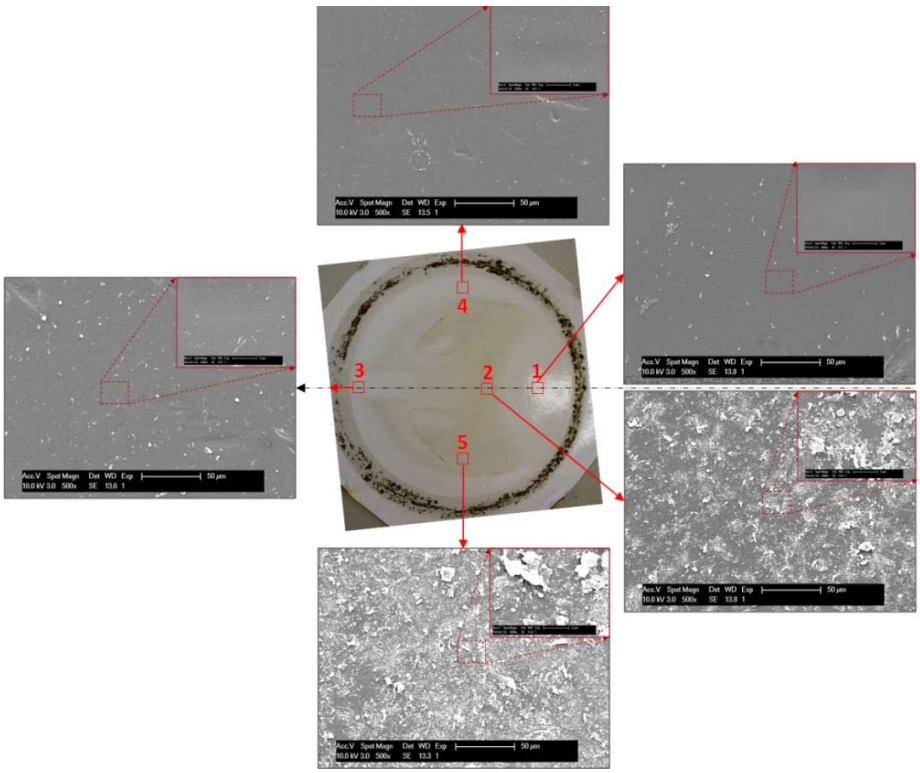

Fig. 4 Digital picture of Sepro NF 6 fouled by 100 ppm humic acid solution and SEM images in different sub-regions

Furthermore, Sepro NF 6 also yielded an outstanding antifouling performance against other foulants as well, i.e., alginate acid and BSA (Supplementary Fig. S1). Noticeably, no significant flux decline was demonstrated for Sepro NF 6 as observed by the low foulant deposition on the membrane surface. For example, only 5.7% flux decline for Sepro NF 6 was observed for a 1000 ppm BSA solution. Therefore, Sepro NF 6 membrane shows a strong potential for advanced treatment of wastewater, due to its excellent antifouling property.

4.2 Effect of feed pH

The solution pH affects the surface charge of the loose NF membrane, which significantly dominates the performance of NF membranes. Furthermore, the pH also has an impact on the structure and properties of humic acids [21]. Fig. 5 shows the effect of pH on the filtration performance of the loose NF membrane used in this study.

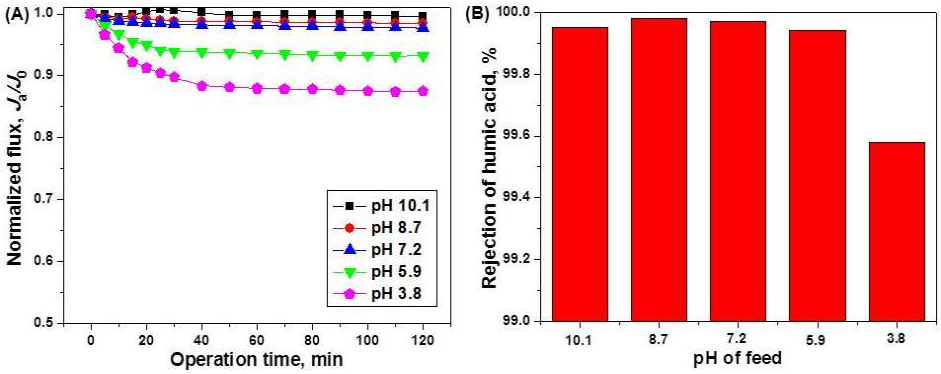

Fig. 5 Effect of pH on flux (A) and solute rejection (B) of Sepro NF 6 in 50 ppm humic acid solution

Fig. 5 shows that the pH of the feed solution significantly influences the flux of the Sepro NF 6 membrane. At the high pH range, negative charges on the membrane surface effectively repel humic acids, which can be dissociated, slightly declining the membrane flux. With the decrease of the feed pH, the membrane surface becomes less negatively charged and the electrostatic attraction between the membrane surface and humic acid is strengthened, resulting in a strong deposition of humic acids and accelerating membrane fouling. A similar phenomenon was observed in previous studies [28,36,37]. Remarkably, at pH 3.8, the foulant-foulant interaction between humic acid molecules was enhanced, and a compact cake layer of humic acid on membrane surface was formed; this was confirmed by SEM images taken at the low velocity zone of the membrane surface (Zones 2 and 5 in Fig. 6). This results in the observed flux decline of 13.0%. However, as demonstrated in the COMSOL simulation, favorable hydraulic conditions can minimize fouling

by humic acids. As shown in Fig. 6, only trace amounts of humic acids were deposited on the membrane surface in the high velocity zones (Zones 1, 3 and 4 in Fig. 6), implying that a good design of the membrane module for benign hydrodynamic conditions are an effective strategy to alleviate membrane fouling for this loose NF membrane.

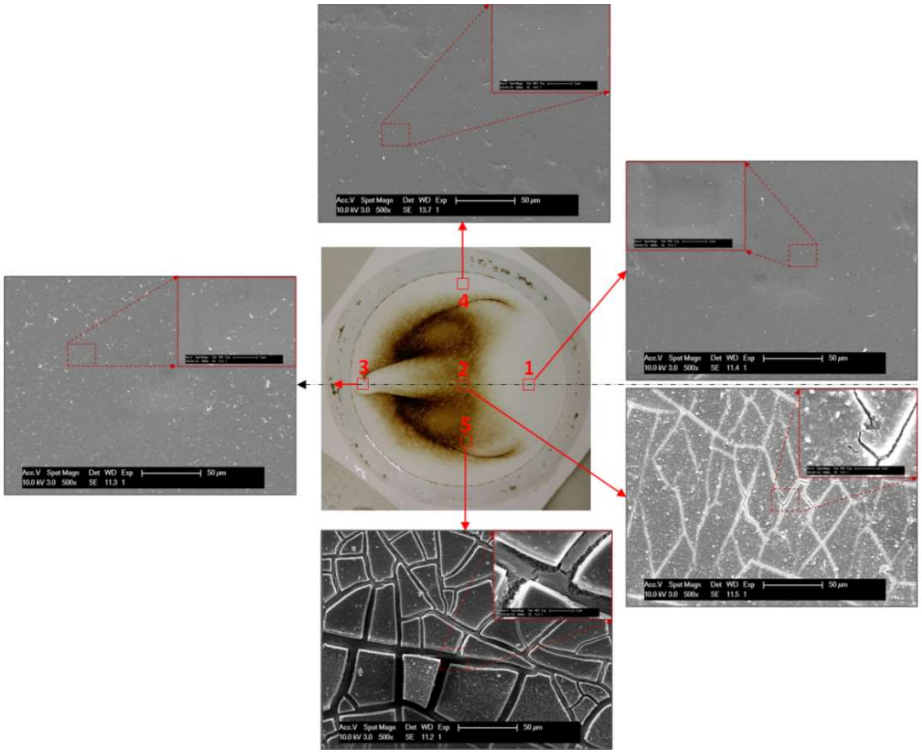

Fig. 6 Digital picture of Sepro NF 6 fouled by 50 ppm humic acid solution at pH 3.5 and SEM images in different sub-regions

On the other hand, the dissociation of humic acid molecules was significantly promoted and small specific molecules composed of humic acids can easily penetrate through the NF membrane at high feed pH (pH = 10.1). With the decrease in feed pH, the rejection of humic acid was slightly boosted. However, the rejection of humic acid drops at the lower pH (pH = 3.8), due to the severe fouling of the membrane surface, which deteriorates the permeate quality. Overall, Sepro NF 6 has a high rejection (>99.6%) for humic acids in the entire pH range.

4.3 Effect of ionic strength

In order to investigate the effect of ionic strength, the filtration performance of humic acids with different NaCl concentrations was conducted (Fig. 7).

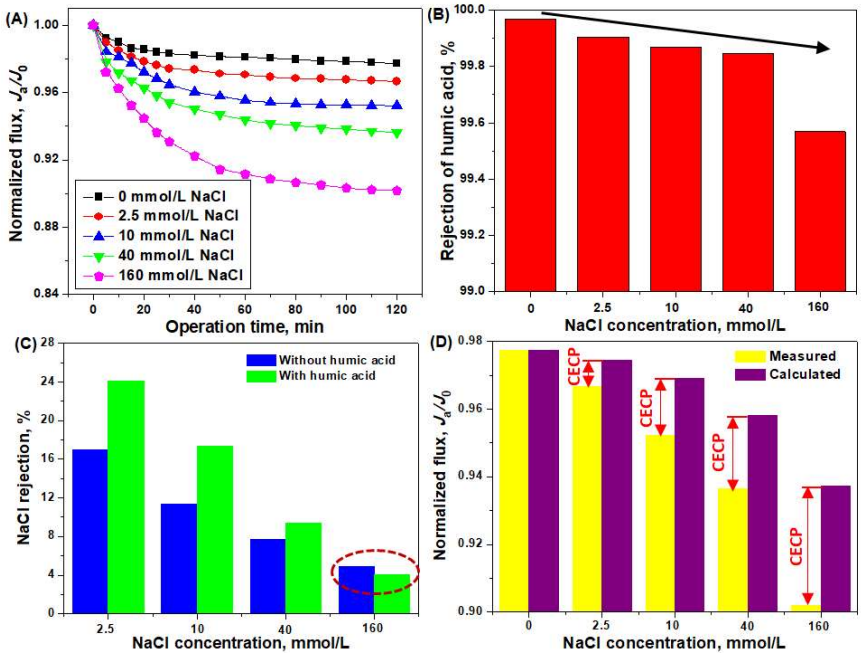

Fig. 7 Filtration performance of Sepro NF 6 at different NaCl concentrations in a 50 ppm humic acid solution. (A): Membrane flux as a function of operation time; (B): humic acid rejection; (C): NaCl rejection; (D): measured flux and theoretical flux.

As shown in Fig. 7(A), the flux of the Sepro NF 6 membrane decreased with the operation time, due to the accumulation of humic acids on the membrane surface. The permeation flux of Sepro NF 6 membrane tended to be constant within 2 h. Expectedly, the flux of Sepro NF 6 in a humic acid solution decreased with NaCl concentration. On one hand, the increase in osmotic pressure difference between feed and permeate sides of the membrane undermines the driving force for permeation with increasing salt concentration. On the other hand, the evaluated concentration of NaCl (thus higher ionic strength) in the humic acid solution diminished the electrostatic repulsive

force between foulant-foulant and foulant-membrane, and resulted in the preferential deposition of humic acid on the membrane surface (Fig. 8), strongly hindering the back diffusion of NaCl from the fouled membrane surface to the bulk solution. This phenomenon, denoted as 'cake-enhanced concentration polarization' (CECP), can further enhance the osmotic pressure of NaCl at the membrane wall, resulting in a severe flux decline (Fig. 7D) [38,39]. As shown in Fig. 8D, the huge gap between the measured flux and the theoretically calculated flux implies that cake-enhance concentration polarization dominates the flux behavior of this loose NF membrane, especially at high ionic strength [8]. In this case, Sepro NF 6 had a regular flux of 0.90 at 0.16 $mol \cdot L^{-1}$ NaCl, which is higher than that (a normalized flux of 0.87) in low pH 3.8. This is mainly due to the fact that Na^+ ions play no significant role for the bridging between humic acid molecules, and solely induce the formation of a loose and porous foulant layer, showing a lower hydraulic resistance (Fig. 8). However, the foulant layer can be clearly observed in Zone 4, which has a moderate flow velocity. This is not consistent with the case at low pH (pH=3.8). Generally, the zeta potential of the fouled membranes depends on the charge properties of humic acid due to the formation of a cake layer [27,40]. Therefore, the zeta potential of the fouled NF membrane increased with NaCl concentration, similar to the case of the humic acid solution (Fig. S2A). This can enhance the electrostatic attraction between membrane surface and humic acid, resulting in the deposition of humic acid in Zone 4 with moderate hydraulic condition in this case. Meanwhile, only a trace amount of humic acid deposited in Zones 1 and 3, indicating that benign hydraulic conditions play a critical role in fouling reduction.

Furthermore, the rejection of humic acids for Sepro NF 6 membrane decreased with the salt concentration (Fig. 7B). This is due to the combined effect of membrane swelling through salting out and the enhanced shielding effect caused by the elevated salt concentration [41-43]. On the

other hand, the rejection of NaCl can be remarkably boosted by the deposition of humic acid with multiple charges on the membrane surface through the enhanced electrostatic repulsion force [27]. It is interesting to note that the gap between the NaCl rejection with and without the presence of humic acid becomes smaller with increasing salt concentration (Fig. 7(C)). This is mainly ascribed to the CECP phenomenon [38,39], since humic acid deposited as macromolecule colloid on the surface of this NF membrane can promote the concentration polarization of NaCl in the porous foulant cake layer, preferentially facilitating the salt permeation.

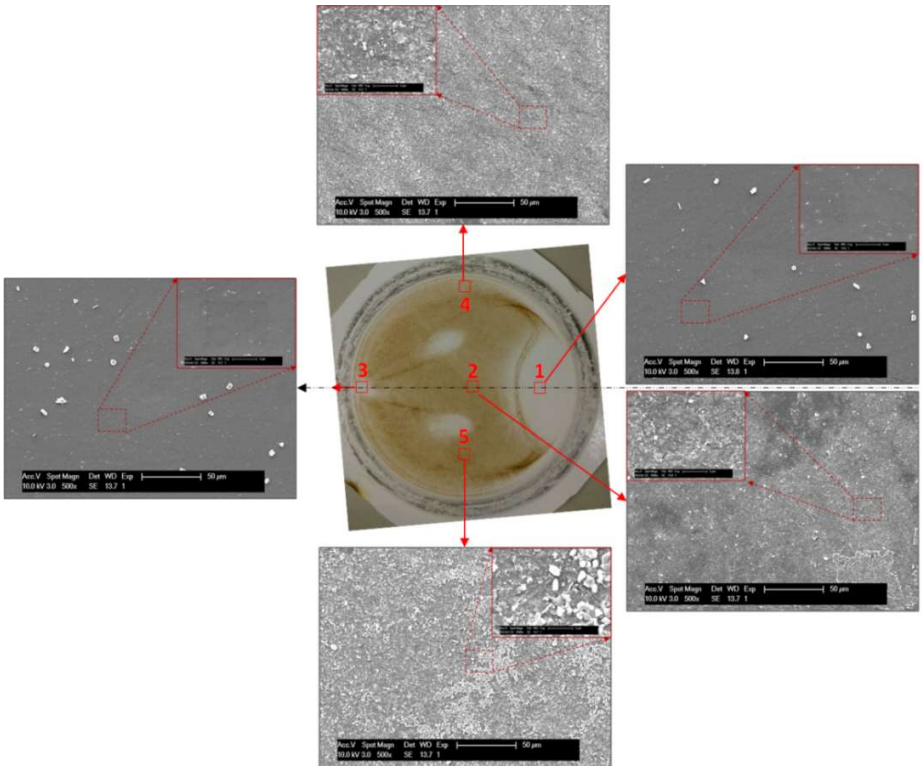

Fig. 8 Digital picture of Sepro NF 6 fouled by 50 ppm humic acid solution with 0.16 mol/L NaCl and SEM images in different sub-regions

4.4 Effect of calcium ion

The bridging of humic acid molecules preferentially occurs in the presence of Ca^{2+} ions, potentially inducing membrane fouling. Fig. 9 shows the fouling behavior of the loose NF membrane with humic acid solution at different Ca^{2+} concentrations.

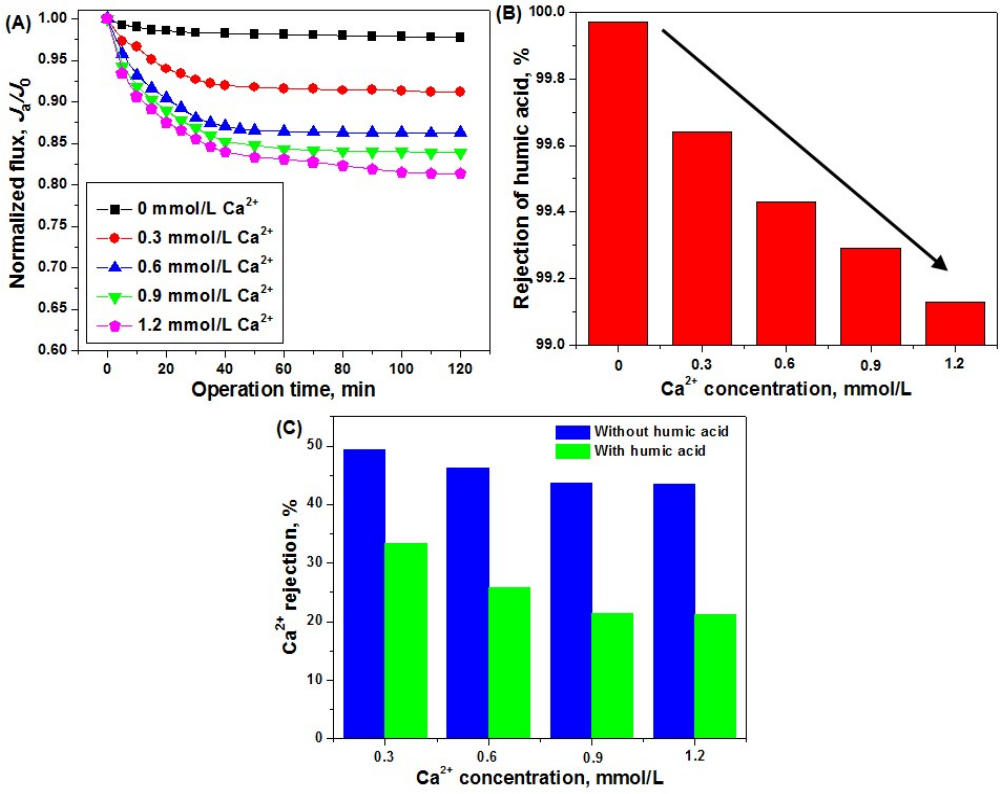

Fig. 9 Filtration performance of Sepro NF 6 membrane at different Ca^{2+} concentrations in a 50 ppm humic acid solution. (A): Membrane flux as a dependence of operation time; (B): humic acid rejection; (C): Ca^{2+} rejection.

As indicated in Fig. 9(A), the flux of the Sepro NF 6 membrane was significantly deteriorated with increasing Ca^{2+} concentrations. Specifically, the Sepro NF 6 membrane had a stable normalized flux of 0.91 when 0.3 mmol·L^{-1} Ca^{2+} ions were present in humic acid solution. While the Ca^{2+} ion concentration increased to 1.2 mmol·L^{-1}, the stable normalized flux of Sepro NF 6 membrane declined to 0.81. This is due to the strong affinity of Ca^{2+} ions to carboxylic groups for both humic acid and the membrane surface, which allows for the formation of strong complexes with humic acid and enhances the collision efficiency between humic acid and the membrane surface for the formation of a compact foulant layer. However, the high-velocity areas, i.e., Zones 1 and 3, have a low propensity for membrane fouling (Fig. 10). The foulant was preferentially deposited on the

membrane surface with low flow velocity, which is similar to the case of a humic acid/NaCl mixed solution. This demonstrates that the hydrodynamic condition on the membrane surface plays a crucial role in alleviating the fouling of this loose NF membrane.

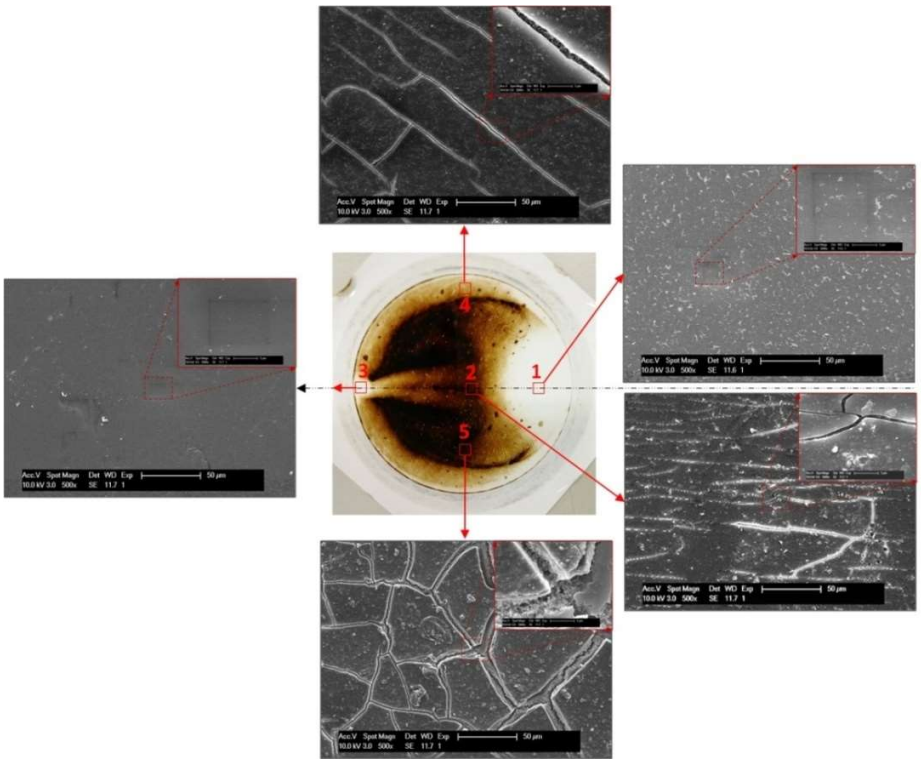

Fig. 10 Digital picture of Sepro NF 6 fouled by 50 ppm humic acid with 1.2 mmol/L Ca^{2+} and SEM images in different sub-regions

Furthermore, the increase in the concentration of Ca^{2+} ions reduces the rejection of humic acid while enhancing the rejection of both the sodium chloride and calcium chloride solutions. For instance, the rejection of humic acid decreased from 99.9% to 99.1% in the presence of 1.2 $mmol \cdot L^{-1}$ Ca^{2+} ions. Two competing phenomena determine the rejection behavior of humic acid under increasing Ca^{2+} ion concentration. On the one hand, the binding of Ca^{2+} ions to the carboxylic groups of Sepro NF 6 membrane and humic acid can further diminish the charge densities of humic acid and the surface of Sepro NF 6 membrane, deteriorating the rejection for

humic acid [44]. On the other hand, the binding of Ca^{2+} ions also can facilitate the formation of complex, resulting in enhanced size exclusion. In this case, the reduced Donnan effect dominates the retention of humic acid over the size exclusion mechanism. This is consistent with previous studies [27,28,44,45]. However, the loose NF membrane shows a consistently high rejection for humic acid. Simultaneously, the Sepro NF 6 membrane is a less effective barrier to Ca^{2+} ions. Specifically, the rejection of Ca^{2+} ions was dropped by 15%~22% in the entire Ca^{2+} concentration range, compared to that in the absence of Ca^{2+} ions.

5. Conclusion

In this work, the flux behavior of a loose NF membrane fouled by humic acid at variable solution compositions (i.e., humic acid concentration, pH, ionic strength, and calcium concentration) was systematically investigated in view of its potential practical application in fractionation of organic matters and salts for resource recovery from wastewater. The Sepro NF 6 membrane showed outstanding antifouling properties against humic acid, BSA, and alginate acid, due to its strong hydrophilicity. However, the fouling caused by foulant deposition was inevitable with the change in composition of the feed solution. A moderate fouling occurred at low pH and high ionic strength through the reduction of the charge density on the surface of the membrane. Specifically, cake enhanced concentration polarization at higher ionic strength was observed, which dominates the flux behavior of the loose NF membrane. On the other hand, the presence of calcium ions induced the rapid evolution of a compact humic acid cake layer through humic acid/Ca^{2+} complexes, substantially deteriorating the membrane flux. However, the hydrodynamic condition shows a more pronounced effect on membrane fouling through SEM observation, which was confirmed by COMSOL simulation in the membrane module. For instance, a trace amount of humic acid deposited on the membrane surface at high crossflow rates, even in the presence of 1.2 $mmol \cdot L^{-1}$

Ca^{2+} ions. These results indicate that the desirable design of the membrane module for benign hydrodynamics can be a critical strategy for mitigating the fouling of loose NF membranes in practical applications.

Acknowledgment

This work was supported by the National Natural Science Foundation of China (Grants No.: 21706035 and 21707018), the Natural Science Foundation of Fujian Province (Grant No.: 2017J01413), the Fujian Agriculture and Forestry University Program for Distinguished Young Scholar (Grant No.: xjq201704) and Fuzhou University (Grants No.: XRC-1622 and 2017T017) for this work. Ultura, USA, is greatly thanked for providing the nanofiltration membrane samples.

References

[1] Mekonnen MM, Hoekstra AY. Four billion people facing severe water scarcity. *Sci Adv* 2016;2:e1500323.

[2] Haddeland I, Heinke J, Biemans H, Eisner S, Flörke M, Hanasaki N, Konzmann M, Ludwig F, Masaki Y, Schewe J, et al. Global water resources affected by human interventions and climate change. *Proc Natl Acad Sci USA* 2014;111:3251-3256.

[3] Han Y, Xu Z, Gao C. Ultrathin graphene nanofiltration membrane for water purification. *Adv Funct Mater* 2013;23:3693-3700.

[4] Guo H, Zhao S, Wu X, Qi H. Fabrication and characterization of TiO_2/ZrO_2 ceramic membranes for nanofiltration, *Micropor Mesopor Mat* 2018;260:125-131.

[5] Shannon MA, Bohn PW, Elimelech M, Georgiadis JG, Marinas BJ, Mayes AM. Science and technology for water purification in the coming decades. *Nature* 2008;452:301-310.

[6] Yu L, Deng J, Wang H, Liu J, Zhang Y. Improved salts transportation of a positively charged

loose nanofiltration membrane by introduction of poly(ionic liquid) functionalized hydrotalcite nanosheets. *ACS Sustain Chem Eng* 2016;4:3292-3304.

[7] Lin J, Ye W, Zeng H, Yang H, Shen J, Darvishmanesh S, Luis P, Sotto A, Van der Bruggen B. Fractionation of direct dyes and salts in aqueous solution using loose nanofiltration membranes. *J Membrane Sci* 2015;477:183-193.

[8] Lin J, Tang CY, Ye W, Sun S, Hamdan SH, Volodin A, Haesendonck CV, Sotto A, Luis P, Van der Bruggen B. Unraveling flux behavior of superhydrophilic loose nanofiltration membranes during textile wastewater treatment. *J Membrane Sci* 2015;493:690-702.

[9] Zhao S, Wang Z. A loose nano-filtration membrane prepared by coating HPAN UF membrane with modified PEI for dye reuse and desalination. *J Membrane Sci* 2017;524:214-224.

[10] Zhu J, Uliana A, Wang J, Yuan S, Li J, Tian M, Simoens K, Volodin A, Lin J, Bernaerts K, Zhang Y, Van der Bruggen B. Elevated salt transport of antimicrobial loose nanofiltration membranes enabled by copper nanoparticles via fast bioinspired deposition. *J Mater Chem A* 2016;4:13211-13222.

[11] Zhu J, Tian M, Hou J, Wang J, Lin J, Zhang Y, Liu J, Van der Bruggen B. Surface zwitterionic functionalized graphene oxide for a novel loose nanofiltration membrane. *J Mater Chem A* 2016;4:1980-1990.

[12] Liu F, Ma B, Zhou D, Zhu L, Fu Y, Xue L. Positively charged loose nanofiltration membrane grafted by diallyl dimethyl ammonium chloride (DADMAC) via UV for salt and dye removal. *React Funct Polym* 2015;86:191-198.

[13] Wang J, Wang Y, Zhu J, Zhang Y, Liu J, Van der Bruggen B. Construction of TiO_2@graphene oxide incorporated antifouling nanofiltration membrane with elevated filtration performance. *J Membrane Sci* 2017;533:279-288.

[14] Zhang Q, Fan L, Yang Z, Zhang R, Liu Y, He M, Su Y, Jiang Z. Loose nanofiltration membrane for dye/salt separation through interfacial polymerization with in-situ generated TiO_2 nanoparticles. *Appl Surf Sci* 2017;410:494-504.

[15] Da X, Wen J, Lu Y, Qiu M, Fan Y. An aqueous sol-gel process for the fabrication of high-flux YSZ nanofiltration membranes as applied to the nanofiltration of dye wastewater. *Sep Purif Technol* 2015;152:37-45.

[16] Lin J, Ye W, Huang J, Ricard B, Baltaru M, Greydanus B, Balta S, Shen J, Vlad M, Sotto A, Luis P, Van der Bruggen B. Toward resource recovery from textile wastewater: Dye extraction, water and base/acid regeneration using a hybrid NF-BMED process. *ACS Sustain Chem Eng* 2015;3:1993-2001.

[17] Cheng XQ, Wang ZX, Zhang Y, Zhang Y, Ma J, Shao L. Bio-inspired loose nanofiltration membranes with optimized separation performance for antibiotics removals. *J Membrane Sci* 2018;554:385-394.

[18] Xing L, Guo N, Zhang Y, Zhang H, Liu J. A negatively charged loose nanofiltration membrane by blending with poly (sodium 4-styrene sulfonate) grafted SiO_2 via SI-ATRP for dye purification. *Sep Purif Technol*. 2015;146:50-59.

[19] Li M, Yao Y, Zhang W, Zheng J, Zhang X, Wang L. Fractionation and concentration of High-Salinity textile wastewater using an ultra-permeable sulfonated thin-film composite. *Environ Sci Technol* 2017;51:9252-9260.

[20] Chidambaram T, Oren Y, Noel M. Fouling of nanofiltration membranes by dyes during brine recovery from textile dye bath wastewater. *Chem Eng J* 2015;262:156-168.

[21] Tang CY, Chong TH, Fane AG. Colloidal interactions and fouling of NF and RO membranes: A review. *Adv Colloid Interfac* 2011;164:126-143.

[22] Wang Y, Tang CY. Protein fouling of nanofiltration, reverse osmosis, and ultrafiltration membranes - the role of hydrodynamic conditions, solution chemistry, and membrane properties. *J Membrane Sci* 2011;376:275-282.

[23] Nghiem LD, Coleman PJ, Espendiller C. Mechanisms underlying the effects of membrane fouling on the nanofiltration of trace organic contaminants. *Desalination* 2010;250:682-687.

[24] Xu P, Bellona C, Drewes JE. Fouling of nanofiltration and reverse osmosis membranes during municipal wastewater reclamation: Membrane autopsy results from pilot-scale investigations. *J Membrane Sci* 2010;353:111-121.

[25] Seidel A, Elimelech M. Coupling between chemical and physical interactions in natural organic matter (NOM) fouling of nanofiltration membranes: Implications for fouling control. *J Membrane Sci* 2002;203:245-255.

[26] Schäfer AI, Fane AG, Waite TD. Nanofiltration of natural organic matter: Removal, fouling and the influence of multivalent ions. *Desalination* 1998;118:109-122.

[27] Tang CY, Kwon Y, Leckie JO. Fouling of reverse osmosis and nanofiltration membranes by humic acid - Effects of solution composition and hydrodynamic conditions. *J Membrane Sci* 2007;290:86-94.

[28] Yoon S, Lee C, Kim K, Fane AG. Effect of calcium ion on the fouling of nanofilter by humic acid in drinking water production. *Water Res* 1998;32:2180-2186.

[29] Lin J, Tang CY, Huang C, Tang YP, Ye W, Li J, Shen J, Van den Broeck R, Van Impe J, Volodin A, Van Haesendonck C, Sotto A, Luis P, Van der Bruggen B. A comprehensive physico-chemical characterization of superhydrophilic loose nanofiltration membranes. *J Membrane Sci* 2016;501:1-14.

[30] Pastagia KM, Chakraborty S, DasGupta S, Basu JK, De S. Prediction of permeate flux and

concentration of two-component dye mixture in batch nanofiltration. *J Membrane Sci* 2003;218:195-210.

[31] Cortés-Juan F, Balannec B, Renouard T. CFD-assisted design improvement of a bench-scale nanofiltration cell. *Sep Purif Technol* 2011;82:177-184.

[32] Shi B, Marchetti P, Peshev D, Zhang S, Livingston AG. Performance of spiral-wound membrane modules in organic solvent nanofiltration - Fluid dynamics and mass transfer characteristics. *J Membrane Sci* 2015;494:8-24.

[33] Moulik S, Vadthya P, Kalipatnapu YR, Chenna S, Sundergopal S. Production of fructose sugar from aqueous solutions: Nanofiltration performance and hydrodynamic analysis. *J Clean Prod* 2015;92:44-53.

[34] Completo C, Semiao V, Geraldes V. Efficient CFD-based method for designing cross-flow nanofiltration small devices. *J Membrane Sci* 2016;500:190-202.

[35] Pawlowski S, Geraldes V, Crespo JG, Velizarov S. Computational fluid dynamics (CFD) assisted analysis of profiled membranes performance in reverse electrodialysis. *J Membrane Sci* 2016;502:179-190.

[36] Mo H, Tay KG, Ng HY. Fouling of reverse osmosis membrane by protein (BSA): Effects of pH, calcium, magnesium, ionic strength and temperature. *J Membrane Sci* 2008;315:28-35.

[37] Zazouli MA, Nasseri S, Ulbricht M. Fouling effects of humic and alginic acids in nanofiltration and influence of solution composition. *Desalination* 2010;250:688-692.

[38] Mahlangu TO, Hoek EMV, Mamba BB, Verliefde ARD. Influence of organic, colloidal and combined fouling on NF rejection of NaCl and carbamazepine: Role of solute-foulant-membrane interactions and cake-enhanced concentration polarisation. *J Membrane Sci* 2014;471:35-46.

[39] Hoek EMV, Elimelech M. Cake-enhanced concentration polarization: A new fouling

mechanism for salt-rejecting membranes. *Environ Sci Technol* 2003;37:5581-5588.

[40] Tang CY, Kwon Y, Leckie JO. Characterization of humic acid fouled reverse osmosis and nanofiltration membranes by transmission electron microscopy and streaming potential measurements. *Environ Sci Technol* 2007;41:942-949.

[41] Freger V, Arnot TC, Howell JA. Separation of concentrated organic/inorganic salt mixtures by nanofiltration. *J Membrane Sci* 2000;178:185-193.

[42] Luo J, Wei S, Su Y, Chen X, Wan Y. Desalination and recovery of iminodiacetic acid (IDA) from its sodium chloride mixtures by nanofiltration. *J Membrane Sci* 2009;342:35-41.

[43] Luo J, Wan Y. Effect of highly concentrated salt on retention of organic solutes by nanofiltration polymeric membranes. *J Membrane Sci* 2011;372:145-153..

[44] Yang L, Zhou J, She Q, Wan MP, Wang R, Chang VWC, Tang CY. Role of calcium ions on the removal of haloacetic acids from swimming pool water by nanofiltration: Mechanisms and implications. *Water Res* 2017;110:332-341..

[45] Hong S, Elimelech M. Chemical and physical aspects of natural organic matter (NOM) fouling of nanofiltration membranes. *J Membrane Sci* 1997;132:159-81.

SUPPLEMENTARY INFORMATION

Theoretical and experimental study of organic fouling of loose nanofiltration membrane

Wenyuan Ye[a], Nicole J. Bernstein[b], Jiuyang Lin[c,d]*, Jeroen Jordens[d], Shuaifei Zhao[e], Chuyang Y. Tang[f], Bart Van der Bruggen[d]

* Corresponding author: linjiuyang@126.com (J. Lin).

[a] *Fujian Provincial Key Laboratory of Soil Environmental Health and Regulation, College of Resources and Environment, Fujian Agriculture and Forestry University, Fuzhou 350002, China*

[b] *Department of Chemical Engineering, Pennsylvania State University, University Park, PA 16802, USA*

[c] *School of Environment and Resources, Qi Shan Campus, Fuzhou University, No. 2 Xueyuan Road, University Town, 350116 Fuzhou, Fujian, China*

[d] *Department of Chemical Engineering, Process Engineering for Sustainable Systems (ProcESS), KU Leuven, Celestijnenlaan 200F, B-3001 Leuven, Belgium*

[e] *Department of Environmental Sciences, Faculty of Science and Engineering, Macquarie University, Sydney, NSW 2109, Australia*

[f] *Department of Civil Engineering, The University of Hong Kong, Pokfulam HW619B, Hong Kong*

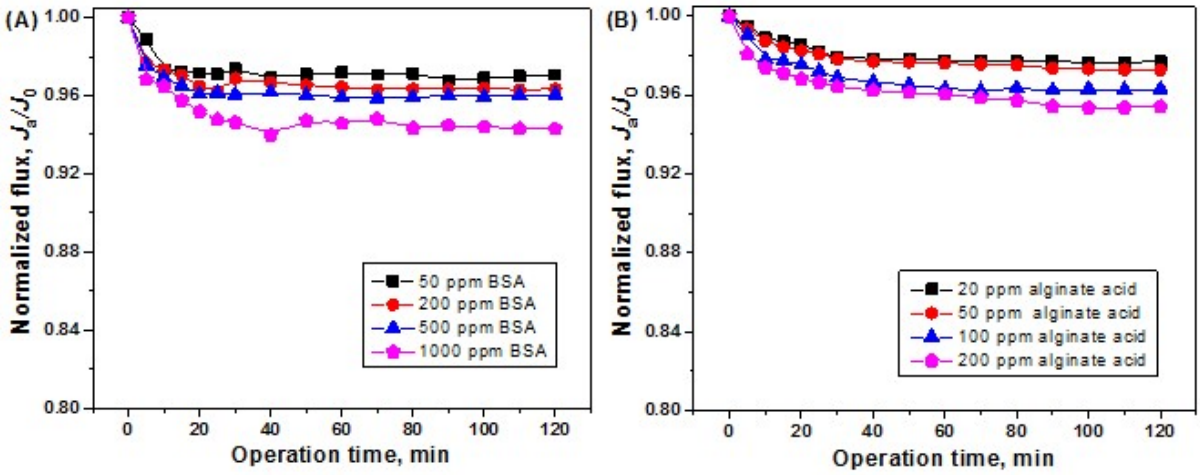

Fig. S1 Flux of Sepro NF 6 in BSA (A) and alginate acid (B) solution with different concentrations

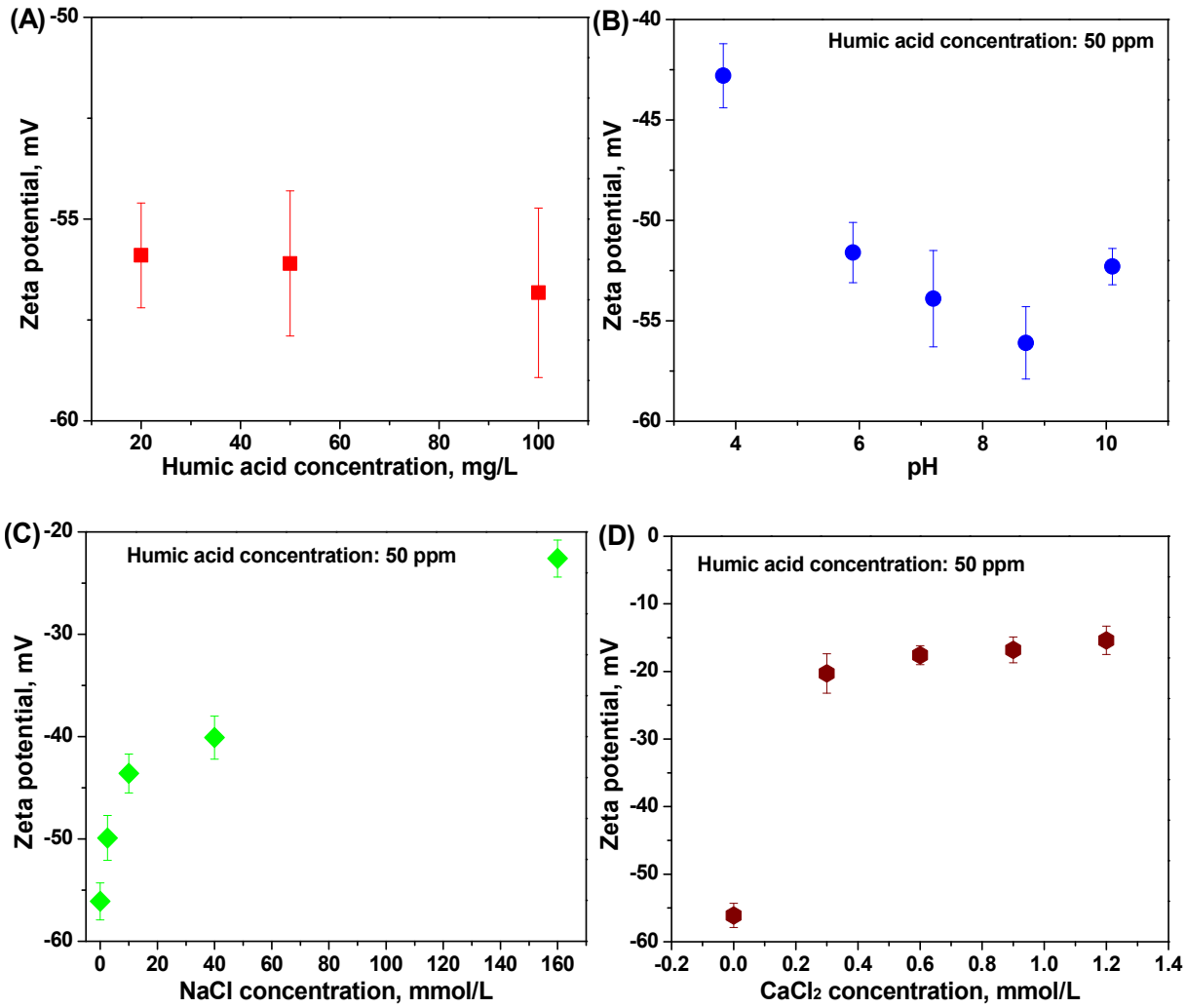

Fig. S2 (A): Zeta potential of humic acid solutions with different concentrations at pH=8.7; (B): Zeta potential of humic acid solutions at different pH values; (C): Zeta potential of humic acids with NaCl addition at pH=8.7; (D): Zeta potential of humic acids with $CaCl_2$ addition at pH=8.7

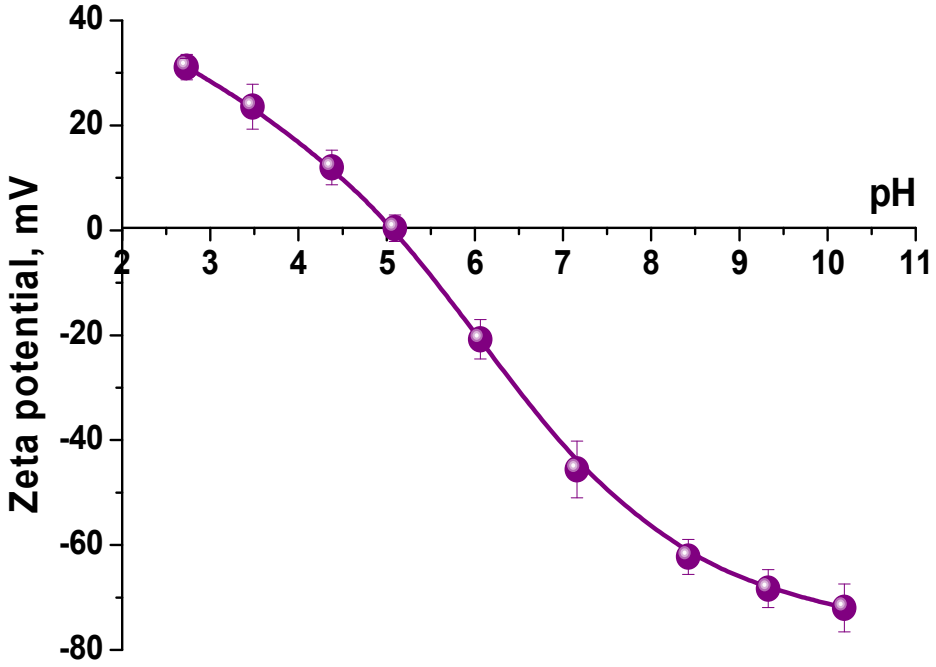

Fig. S3 Zeta potential of Sepro NF 6 membrane versus pH value [1]

References:

[1] Lin J, Tang CY, Huang C, Tang YP, Ye W, Li J, Shen J, Van den Broeck R, Van Impe J, Volodin A, et al. A comprehensive physico-chemical characterization of superhydrophilic loose nanofiltration membranes. *J Membrane Sci* 2016;501:1-14.